

Comparative Study of New Quinoxaline Derivatives Towards Corrosion of Copper in Nitric Acid

A. Zarrouk¹, B. Hammouti^{1,*}, R. Touzani^{1,2}, S.S. Al-Deyab³, M. Zertoubi⁴, A. Dafali¹, S. Elkadiri¹

¹ LCAE-URAC18, Faculté des Sciences, Université Mohammed I^{er} B.P. 717, 60000 Oujda, Morocco.

² LCAE-URAC18, Faculté Polydisciplinaire, Université Mohammed Premier, Nador, Morocco.

³ Department of Chemistry, College of Science, King Saud University, B.O. 2455, Riaydh 11451, Saudi Arabia

⁴ Laboratoire LEMI, Faculté des sciences, Université Ain Chock casablanca, B.P 5366 Maarif Casablanca, Morocco..

*E-mail: hammoutib@gmail.com

Received: 14 July 2011 / Accepted: 7 September 2011 / Published: 1 October 2011

The inhibitive effect three quinoxalines derivatives named (2Z)-1-(4-chlorophenyl)-2-[(3E)-3-[2-(4-chlorophenyl)-2-oxoethylidene]-3,4-dihydroquinoxalin-2(1H)-ylidene]ethanone (Q4), (2Z)-2-[(3E)-3-(2-oxo-2-phenylethylidene)-3,4-dihydroquinoxalin-2(1H)-ylidene]-1-phenylethanone (Q5) and (Z)-2-[(E)-3-(2-oxo-2-phenylethylidene)-3,4-dihydroquinoxalin-2(1H)-ylidene]-1-phenylethanone (Q6) on the corrosion of copper in 2 M HNO₃ has been investigated at 303 K. The study was carried out using weight loss measurements, potentiodynamic polarisation and electrochemical impedance spectroscopy (EIS) methods). Results obtained show that Q4 is the best inhibitor and its inhibition efficiency (E %) increases with the increase of inhibitor concentration and reached up to 90 % for Q4 at 10⁻³ M. Potentiodynamic polarisation studies clearly reveal that the presence of inhibitors does not change the mechanism of hydrogen evolution and that they act as mixed inhibitors with predominance at cathodic range.

Keywords: Copper, Nitric acid, Inhibitors, Quinoxalines, Polarisation curves, Impedance.

1. INTRODUCTION

The use of metallic materials plays a very important role in diverse fields of life, industry and, consequently, in economics. Their protection from corrosion is the major goal. In this optic, the studying the processes of corrosion continues to increase the life of metal use and save money [1-4]. Among the different techniques, the use of corrosion inhibitors is widely practiced. The mechanism of organic corrosion inhibitors work is usually related to adsorption phenomenon against heteroatoms,

aromatic rings... called active centre of adsorption. Two possible mode of adsorption are introduced: physical adsorption and/or chemical adsorption. The inhibition, normally considered by corrosion scientists is the relation between the molecular structure and corrosion inhibition efficiency [5-9]

Quinoxalines and its derivatives are among compounds, which inhibit the corrosion of iron and aluminium in HCl aqueous solution [10-18].

The objective here is to test three quinoxalines derivatives synthesized as corrosion inhibitors of copper in 2M HNO₃. Measurements were carried out with potentiokinetic polarization and electrochemical impedance spectroscopy (EIS) measurements and gravimetric method. The chemical structures of the studied quinoxalines derivatives are given in Figure 1.

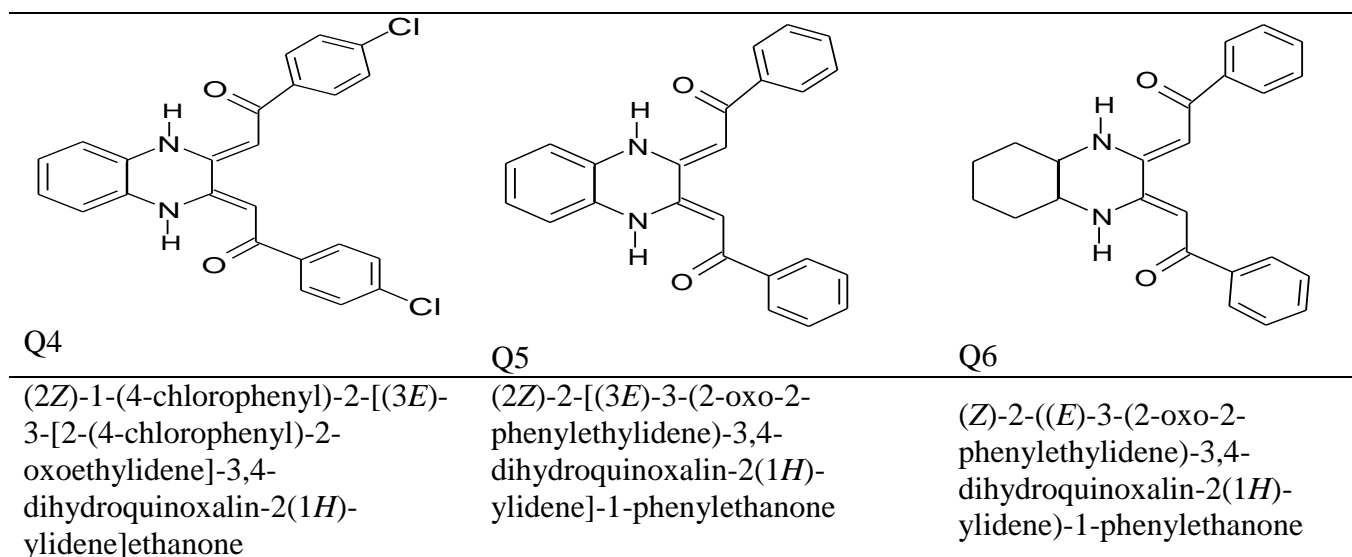


Figure 1. The proposed structure of the studied quinoxalines derivatives.

2. EXPERIMENTAL DETAILS

2.1. Materials and reagents

Copper strips containing 99.5 wt.% Cu, 0.001wt.% Ni, 0.019 wt.% Al, 0.004 wt.% Mn, 0.116 wt.% Si and balance impurities were used for electrochemical and gravimetric studies. The Copper samples were mechanically polished using different grades of emery paper, washed with double distilled water, and dried at room temperature. Appropriate concentration of aggressive solutions used (2 M HNO₃) was prepared using double distilled water.

2.2. Synthesis

Preparation of 2,3-disubstituted quinoxaline compounds in most cases involves the condensation of diketone [19] or diethyl oxalate compounds [20] with *o*-phenylenediamine. One

useful route to 2,3-difunctionalized quinoxalines is the condensation reaction of diketones with various 1,2-diaminocompounds. Disubstituted hexan-1,3,4,6-tetraones have proven to be versatile reagents employed with substituted hydrazines in the synthesis of bipyrazole ligands [20] and have been used for the synthesis of 2,3-difunctionalized quinoxalines Q4-Q6 [21-24]. A few synthetic methods are available in the literature but none of them are very convenient. Furthermore, hexan-1,3,4,6-tetraone is not commercially available. Accordingly, we have improved the method described by Finar [19]. Our method is shorter (a 1-day reaction at ambient temperature), the yield is excellent (80-85 %) and the method is delightfully simple as well as convenient compared to other methods in the literature.

2.3. Electrochemical measurements

❖ *Electrochemical cell*

The electrolysis cell was Pyrex of cylinder closed by cap containing five openings. Three of them were used for the electrodes. The working electrode was copper with the surface area of 0.28 cm². Before each experiment, the electrode was polished using emery paper until 2000 grade. After this, the electrode was cleaned ultrasonically with distillate water. A saturated calomel electrode (SCE) was used as a reference. All potentials were given with reference to this electrode. The counter electrode was a platinum plate of surface area of 1 cm².

The aggressive medium used here is 2 M HNO₃ solutions were prepared with concentrated HNO₃ and distilled water. The molecule structures of quinoxalines tested are shown in Fig. 1. The concentration range of this compounds was 10⁻⁶ to 10⁻³ M.

❖ *Polarization measurements*

The working electrode was immersed in test solution during 30 minutes until a steady state open circuit potential (E_{ocp}) was obtained. The polarization curve was recorded by polarization from -150 mV to 150 mV under potentiodynamic conditions corresponding to 1 mV/s (sweep rate) and under air atmosphere. The potentiodynamic measurements were carried out using Tacussel Radiometer PGZ 301, which was controlled by a personal computer.

❖ *EIS measurements*

The electrochemical impedance spectroscopy measurements were carried out using a transfer function analyser (Tacussel Radiometer PGZ 301), with a small amplitude ac. Signal (10 mV rms), over a frequency domain from 100 KHz to 10 mHz at 303 K and an air atmosphere. The polarization resistance R_p , is obtained from the diameter of the semicircle in Nyquist representation.

2.4. Weight loss measurements

Gravimetric experiments were carried out in a double walled glass cell. The solution volume was 50 cm³; the temperature of 303 K was controlled thermostatically. The weight loss of copper in

2 M HNO₃ with and without the addition of inhibitor was determined after immersion in acid for 1 h. The copper specimens were rectangular in the form (2 cm × 2 cm × 0.20 cm).

3. RESULTS AND DISCUSSION

3.1. Synthesis and characterization

3.2. Polarisation curves

Figs. 2-4 represent the potentiodynamic polarization curves of copper in 2M HNO₃ without and with different concentrations of inhibitor Q4, Q5 and Q6, respectively, at 303 K. The data show that, the addition of inhibitors affects slightly the corrosion potential (E_{corr}) to more cathodic values. The electrochemical parameters (I_{corr} , E_{corr} and b_c) are given in Table 1. $E_I\%$ was calculated using the equation 1:

$$E_I \% = \frac{I_{corr}^0 - I_{corr}}{I_{corr}^0} \times 100 \tag{1}$$

I_{corr}^0 and I_{corr} are the corrosion current density in the absence and presence of inhibitor.

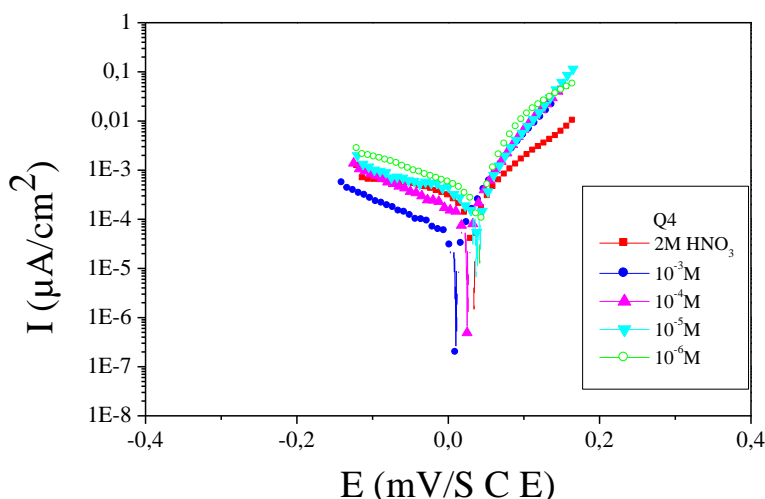


Figure 2. Polarisation curves for Copper in 2M HNO₃ containing different concentrations of Q4

It is obvious that the cathodic Tafel slope (b_c) varies in the presence of each inhibitor. The decrease of I_{corr} indicates that the addition of quinoxalines inhibits the corrosion process by decreasing the surface area for corrosion. The mechanism of corrosion is affected by merely blocking the reaction sites of the metal surface with changing the cathodic reaction mechanisms. In the anodic domain, the presence of Q4-6 increases the anodic current density. This result indicates that the compounds

accelerate the dissolution of copper in nitric acid solution. These inhibitors may be classified as cathodic type inhibitors. It is seen that the addition of various inhibitors decreases I_{corr} significantly for all the studied concentrations, due to increase in the blocked fraction of the electrode surface by adsorption. The cathodic current versus potential curves gave rise to Tafel lines indicating that the hydrogen evolution reaction is activation-controlled, b_c values is slightly modified and then the addition of inhibitors modifies the mechanism of the proton discharge reaction. The efficiency obtained shows that the inhibitory effect of quinoxalines tested increases in the following sequence:

$$Q4 > Q5 > Q6$$

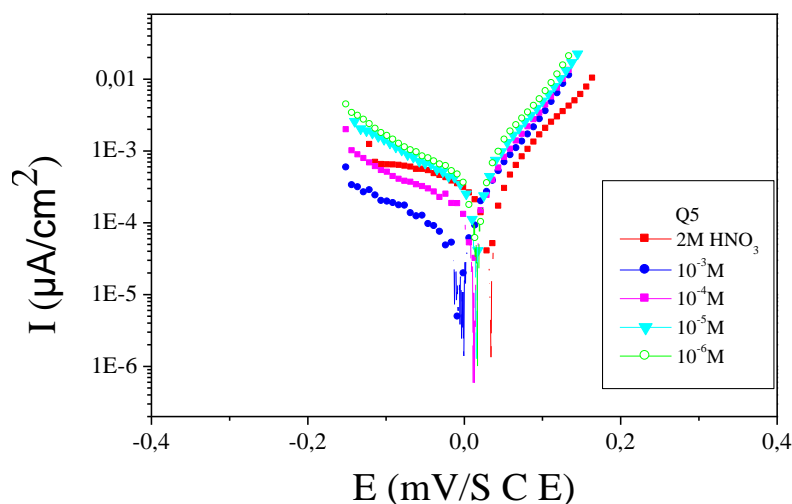


Figure 3. Polarisation curves for Copper in 2M HNO₃ containing different concentrations of Q5

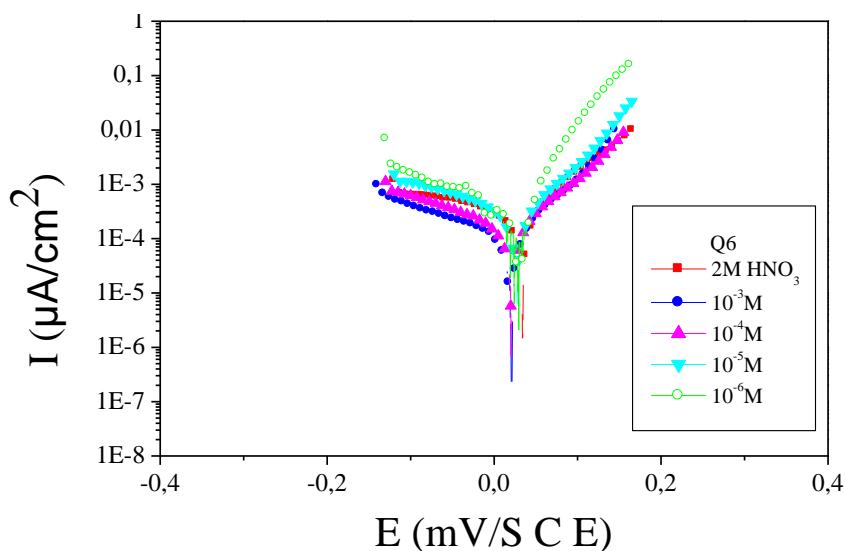


Figure 4. Polarisation curves for Copper in 2M HNO₃ containing different concentrations of Q6

3.2.3. Electrochemical impedance spectroscopic studies

Figure 5 presents the Nyquist diagrams obtained in the absence and presence of Q4 at different concentrations. The impedance parameters calculated are given in Table 2. The charge-transfer resistance values (R_{ct}) were calculated from the difference in impedance at lower and higher frequencies. To obtain the double-layer capacitance (C_{dl}), the frequency at which the imaginary component of the impedance is maximum ($-Z_{imax}$) is found and C_{dl} values were obtained from the equation 2:

$$f(-Z_{imax}) = \frac{1}{2\pi C_{dl} R_t} \tag{2}$$

Table 1. Polarisation data of Copper in 2M HNO₃ without and with addition of inhibitors at 303 K.

	Conc (M)	E_{corr} (mV/SCE)	$-b_c$ (mV/dec)	I_{corr} ($\mu A/cm^2$)	IE (%)
HNO ₃	2	34	304	365.1	-
Q4	10 ⁻³	11	153	047.1	<u>87.1</u>
	10 ⁻⁴	25	152	117.3	67.8
	10 ⁻⁵	34	223	277.4	24.0
	10 ⁻⁶	41	176	311.6	14.6
Q5	10 ⁻³	-04	182	062.2	<u>82.9</u>
	10 ⁻⁴	11	185	126.2	65.4
	10 ⁻⁵	14	167	291.8	20.0
	10 ⁻⁶	15	178	328.5	10.0
Q6	10 ⁻³	20	190	102.5	<u>71.9</u>
	10 ⁻⁴	20	189	153.8	57.8
	10 ⁻⁵	26	204	290.7	20.3
	10 ⁻⁶	26	193	315.0	13.7

In this case, the inhibition efficiency is calculated using charge transfer resistance from equation 3:³³

$$E_z \% = \frac{R_{t(inh)} - R_t}{R_{t(inh)}} \times 100 \tag{3}$$

where $R_{t(inh)}$ and R_t are the charge transfer resistance in the presence and absence of Q4, respectively.

It is evident from Fig. 5 that, the Nyquist plots of copper show a depressed semi circular shape and only one time constant was observed in Bode diagrams (Fig. 6). This observation indicates that the corrosion of Cu in 2M HNO₃ solution is mainly controlled by a charge transfer process [25].

The presence of one phase maximum at intermediate frequencies indicates the presence of one time constant corresponding to the impedance of the formed protective film. In Bode plots for pure capacitive behaviour the slope of $\text{Log}(-Z_i)$ vs. $\text{Log} f$ relation should be -1 . In present work, the resulting value is approximately -0.99 , which indicate a capacitive behaviour of copper electrode under the experimental conditions [26].

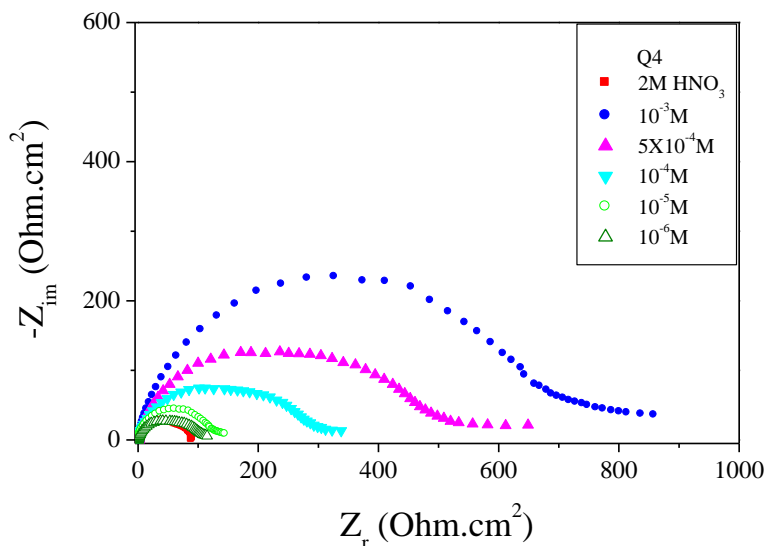


Figure 5. Nyquist diagrams Copper in 2M HNO₃ without and with different concentrations of Q4

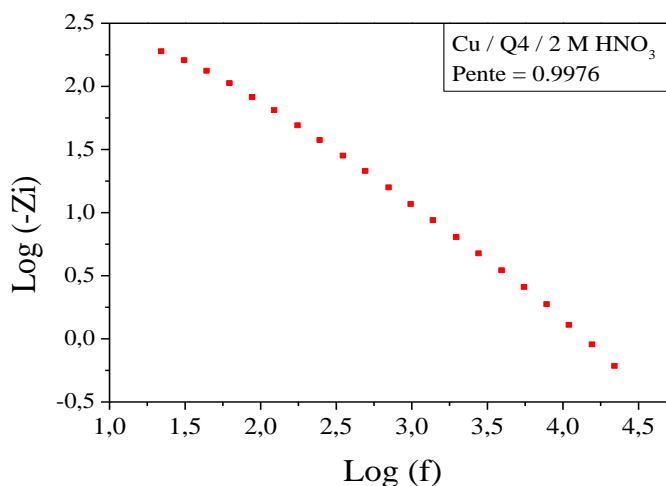


Figure 6. Variation of $\text{Log}(-Z_i)$ as function of logarithm of frequency of Cu / 10^{-3} M Q4 / 2 M HNO₃

The appearance of Nyquist plots remained the same, their diameter proportionally to R_t increased after the addition of Q4 to the aggressive solution. This increase was more and more

pronounced with increasing inhibitor concentration which indicates that the adsorption of inhibitor molecules occurs on the metal surface (Fig. 7).

Table 2. EIS parameters for the Copper corrosion in 2M HNO₃ containing different concentrations of Q4.

	Conc (M)	R _t (Ω.cm ²)	f _{max} (Hz)	C _{dl} (μF/cm ²)	E _{Rt} (%)
HNO ₃	2	091.41	15.82	110.11	-
	10 ⁻³	700.94	04.46	050.87	86.9
	5×10 ⁻⁴	495.16	05.61	057.24	81.5
Q4	10 ⁻⁴	289.74	07.14	076.94	68.4
	10 ⁻⁵	122.83	12.50	104.16	25.6
	10 ⁻⁶	107.30	12.50	118.72	14.8

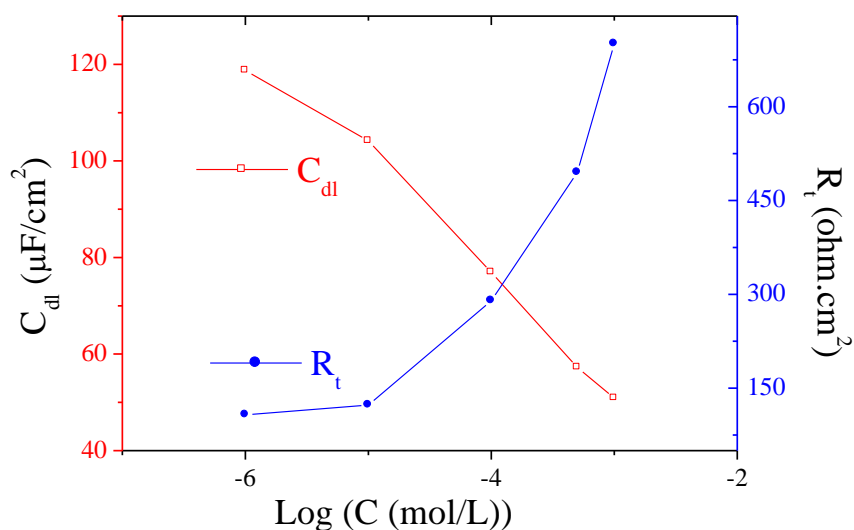


Figure 7. Evolution of transfer resistance and capacitance as function of logarithm of Q4 concentration

The Nyquist plots are not perfect semicircles and generally attributed to the frequency dispersion as well as to the inhomogeneities of surface and mass transport resistant [27-29]. Furthermore, C_{dl} decreases with increase of the concentration of inhibitor (Fig. 7). This phenomenon is generally related to the adsorption of organic molecules on the metal surface and then leads to a decrease in the local dielectric constant and/or an increase in the thickness of the electrical double layer [30].

$$C_{dl} = \frac{\epsilon_o \epsilon}{\delta} S \tag{4}$$

where δ is the thickness of the protective layer, S is the electrode area, ϵ_0 the vacuum permittivity of vide and ϵ is dielectric constant of the medium.

A low capacitance may result if water molecules at the electrode interface are largely replaced by organic inhibitor molecules through adsorption [31]. The larger inhibitor molecules also reduce the capacitance through the increase in the double layer thickness [32].

3.2.1 Gravimetric measurements

The effect of addition of Q4, Q5 and Q6 at different concentrations on the corrosion of copper in 2M HNO₃ solution was studied by weight loss at 1 h. Table 3 gathers the values deduced of W_{corr} and $E_w\%$. In this case, the inhibition efficiency ($E_w\%$) is determined by the equation 5:

$$E_w\% = \frac{(W_{\text{corr}}^0 - W_{\text{corr}})}{W_{\text{corr}}^0} \times 100 \quad (5)$$

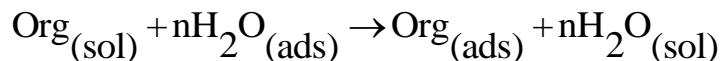
where W_{corr} and W_{corr}^0 are the corrosion rates of copper with and without inhibitor, respectively.

Gravimetric measurement shows that the corrosion decreases in the presence of Q4, Q5 and Q6. The inhibitive action is better expressed by the inhibition efficiency which increases with inhibitor concentration to reach 90.2% for Q4, 88.4% for Q5 and 77.6% for Q6 at 10⁻³M (Table 3). Then all inhibitors studied inhibit the corrosion of copper in 2M HNO₃, but the inhibitor Q4 is found to be more effect.

Table 3. Gravimetric results of copper in 2M HNO₃ without and with addition of inhibitors at 303 K.

Inhibitors	C (M)	W (mg/cm ² .h)	E _w (%)
	Blank	1.7800	-
	10 ⁻³	0.1739	90.2
	5×10 ⁻⁴	0.2409	86.5
Q4	10 ⁻⁴	0.5244	70.5
	5×10 ⁻⁵	0.9086	49.0
	10 ⁻⁵	1.3448	24.5
	10 ⁻⁶	1.4872	16.5
	10 ⁻³	0.2059	88.4
	5×10 ⁻⁴	0.2726	84.7
Q5	10 ⁻⁴	0.5004	71.9
	5×10 ⁻⁵	0.8587	51.8
	10 ⁻⁵	1.3726	22.9
	10 ⁻⁶	1.4954	16.0
	10 ⁻³	0.3994	77.6
	5×10 ⁻⁴	0.4921	72.3
Q6	10 ⁻⁴	0.6353	64.3
	5×10 ⁻⁵	0.9137	48.7
	10 ⁻⁵	1.4042	21.1
	10 ⁻⁶	1.5329	13.9

The adsorption process of inhibitor is regarded as a displacement reaction where the adsorbed water molecule is being removed from the surface of metal [33]:



$\text{Org}_{(\text{sol})}$ and $\text{Org}_{(\text{ads})}$ are the organic molecules in the aqueous solution that adsorbed to the metal surface.

Under the assumptions that the corrosion of the covered parts of the surface is equal to zero and that corrosion takes place only on the uncovered parts of the surface (i.e., inhibitor efficiency is due mainly to the blocking effect of the adsorbed species), the degree of surface coverage Θ has been estimated from the chemical and electrochemical techniques employed in this study as follows [28]:

$$\Theta = E(\%)/100$$

(assuming a direct relationship between surface coverage and inhibition efficiency) [34].

Adsorption isotherms are very important in determining the mechanism of organic electrochemical reactions. The most frequently used adsorption isotherms are Langmuir, Temkin and Frumkin with the general formula:

$$f(\Theta, x) \exp(-2a \Theta) = KC \quad (10)$$

In nitric acid solution, the organic compound follows the Langmuir adsorption isotherm. This is as follows:

$$\frac{\Theta}{1 - \Theta} = KC \quad (11)$$

Rearranging this equation gives:

$$\frac{C}{\Theta} = \frac{1}{K} + C \quad (12)$$

where C is the concentration of inhibitor, K is the adsorptive equilibrium constant, and Θ is the surface coverage.

The linear regressions between C/Θ and C indicate that the adsorption of inhibitors onto copper surface obeys well the Langmuir adsorption isotherm (Fig. 8). Adsorption parameters of quinoxalines tested on copper in 2M HNO_3 at 303 K are gathered in Table 4.

The linear correlation coefficients (r) are almost equal to 1.000 and all the slopes are very close to 1.00.

In addition, it could be found (Table 4) that the adsorption coefficient. The standard adsorption free energy ($\Delta G_{\text{ads}}^\circ$) was obtained according to the following equation:

$$K = \frac{1}{55.5} \exp\left(-\frac{\Delta G_{ads}^\circ}{RT}\right) \tag{14}$$

Table 4. Adsorption parameters of quinoxalines tested on copper in 2M HNO₃ at 303 K.

	R ²	Slope	K	ΔG [°] _{ads} (kJ.mol ⁻¹)
Q4	0.9995	1.080	33715.4	-36.38
Q5	0.9996	1.108	36114.1	-36.56
Q6	0.9994	1.268	33281.2	-36.35

Values of ΔG[°]_{ads} were found to be around -36 kJ.mol⁻¹. It is usually accepted that the values of ΔG[°]_{ads} around -20 kJ.mol⁻¹ or lower indicates the electrostatic attraction between the charged metal surface and charged organic molecules in the bulk of the solution. Those around -40 kJ.mol⁻¹ or higher involve charge sharing or charge transfer between the metal and the organic molecules [35]. The negative value of ΔG[°]_{ads} obtained reveals the spontaneity of adsorption process [36] and at the same time indicates physical adsorption of quinoxalines molecules on copper surface.

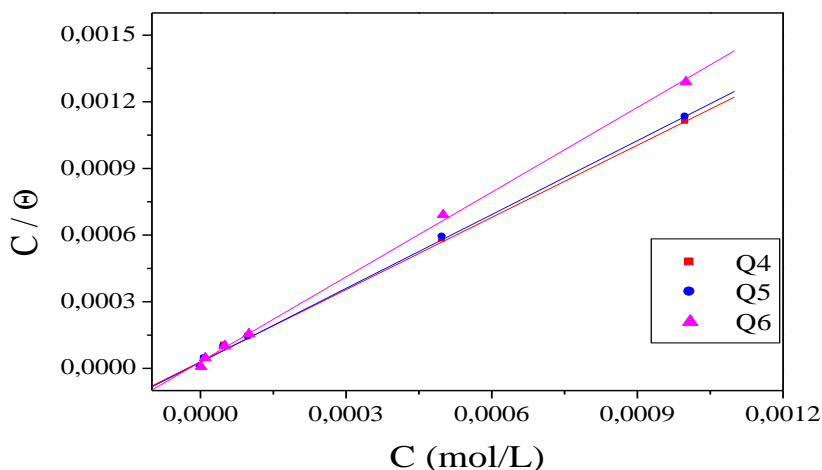


Figure 8 . Langmuir isotherm for the adsorption of quinoxalines on the surface of copper in 2M HNO₃

3.3 Inhibition mechanism

Quinoxalines and its derivatives show good inhibition efficiencies for copper corrosion in nitric acid. The inhibiting action of these inhibitors is attributed to their adsorption to the copper/solution interface. It has been observed that adsorption depends mainly on certain physico-chemical properties of the inhibitor group. Like functional groups, aromaticity, electron density at the donor atoms and π-

orbital character of donating electrons and also the presence of hetero-atom such as N and O, as well as multiple bonds in their molecular structure, are assumed to be active centres of adsorption [37].

Q4 gives the best inhibition efficiency among Q5 and Q6. The high inhibition efficiency of Q4 is due to the presence of the chloro group in Para position of the phenyl ring which increase the electron density on the quinoxaline structure in Q4 more than Q5 and Q6. Adsorption of Quinoxalines derivatives can be described by two main types of adsorption: physisorption and chemisorption. Physisorption requires the presence of both the electrically charged surface of the metal and charged species in solution. A chemisorption process involves charge sharing or charge-transfer from the inhibitor molecules to the metal surface to form a coordinate type of a bond. This is possible in the case of a positive as well as a negative charge of the surface.

The presence of a cuprous as well as cupric ions with a vacant d-orbital and the presence of quinoxaline derivatives with heteroatoms (N and O-atoms) and aromatic rings having relatively loosely bound electrons and/or heteroatoms with lone pairs of electrons are necessary for the adsorption process to occur [38]. Generally, the two types of mechanisms of inhibition were proposed. One was the formation of complexes with copper ions (Cu^+ , Cu^{2+}) depending on the applied conditions. The other was the chemical adsorption of quinoxaline derivatives on copper surfaces. Similarly to adsorption of benzotriazole derivatives, adsorption of quinoxaline derivatives might induce the formation of semiconductive copper oxides. This was possibly responsible for the improvement of corrosion resistance. Q4, Q5 and Q6 are organic bases which protonize in acid medium, thus quinoxaline derivatives become cations (protonated N-atoms), existing in equilibrium with the corresponding molecular form (unprotonated N-atoms). Possible physical adsorption on negatively charged copper surface can be occurred. Adsorption in this case is assisted by hydrogen bond formation between quinoxaline derivatives and the intermediates. The type of intermediates that formed on Cu surface in molar nitric acid can be explained according to the copper potential-pH diagram (pourbaix diagram).

It is seen that a stable Cu_2O is formed only in acidic solution of pH over 2. Nevertheless, since the proton H^+ is continuously consumed to the hydrogen gas H_2 during the Cu dissolution, the pH value near the Cu electrode in molar nitric acid instantaneously jump from 1 to greater values. Thus it is acceptable to think that Cu_2O can be metastably formed on the Cu surface even at Open circuit potential in molar nitric acid [39]. The presence of Cu_2O may facilitate adsorption via H-bond formation.

Another possible mechanism, therefore may be adsorption assisted by hydrogen bond formation between protonated and unprotonated N atoms in the molecule and the oxidized surface (Cu_2O) species. The latter should be more prevalent for protonated N atoms, because the positive charge on N is conducive to the formation of hydrogen bonds. Unprotonated N atoms may adsorb by direct chemical adsorption or by hydrogen bonding to a surface oxidized species. The extent of adsorption by the respective modes depends on the nature of the metal surface. The adsorption layer acts as an additional barrier to the corrosive attack and enhances the performance of the passive layer as a result [40].

4. CONCLUSION

On the basis of these results, it can be seen that:

- Q4, Q5 and Q6 inhibit the corrosion of copper in 2M HNO₃. Q4 is found to be more effective.
- The inhibition efficiency increases with increasing of inhibitor concentration to attain a maximum value of 90.2 % for inhibitor Q4 at 10⁻³ M.
- They act principally as cathodic inhibitors.
- Quinoxalines adsorb on the copper surface according to the Langmuir isotherm.

ACKNOWLEDGEMENTS

Prof. Hammouti and Prof. Al-Deyab extend their appreciation to the Deanship of Scientific Research at King Saud University for funding the work through the research group project.

References

1. A.P. Srikanth, T. G. Sunitha, V. Raman, S. Nanjundan, N. Rajendran, *Mater. Chem. Phys.* 103 (2007) 241.
2. K. Tebbji, N. Faska, A. Tounsi, H. Oudda, M. Benkaddour, *Mater. Chem. Phys.* 106 (2007) 260.
3. L. Herrag, B. Hammouti, A. Aouniti, S. El Kadiri, R. Touzani, *Acta Chim. Slov.* 54 (2007) 419.
4. M. Bouklah, A. Attayibat, B. Hammouti, A. Ramdani, S. Radi, M. Benkaddour, *Appl. Surf. Sci.* 240 (2005) 341.
5. M. Zerfaoui, H. Oudda, B. Hammouti, S. Kertit, M. Benkaddour, *Prog. Org. Coat.* 51 (2004) 134.
6. M.L. Free, *Corros. Sci.* 46 (2004) 3101.
7. R. Salghi, L. Bazzi, B. Hammouti, A. Bendou, E. Ait Addi, S. Kertit, *Prog. Org. Coat.* 51 (2004) 113.
8. Nageh K. Allam, *Appl. Surf. Sci.* 253 (2007) 4570.
9. Qi Zhang, Zhinong Gao, Feng Xu, Xia Zou, *Colloids and Surfaces A: Physicochemical and Engineering Aspects* 380 (2011) 191.
10. A. Zarrouk, A. Dafali, B. Hammouti, H. Zarrok, S. Boukhris, M. Zertoubi, *Int. J. Electrochem. Sci.* 5 (2010) 46.
11. I. El Ouali, B. Hammouti, A. Aouniti, Y. Ramli, M. Azougagh, E. M. Essassi, M. Bouachrine, J. *Mater. Environ. Sci.* 1 (2010) 1.
12. M. Elayyachy, B. Hammouti, A. El Idrissi, A. Aouniti, *Port. Electrochim. Acta.* 29 (2011) 57.
13. B. Hammouti, A. Zarrouk, S. S. Al-Deyab, *Oriental J. Chem.* 27 (2011) 23.
14. I.B. Obot, N. O. Obi-Egbedi, N.W. Odozi, *Corros. Sci.* 52 (2010) 923 .
15. I.B. Obot, N. O. Obi-Egbedi, *Mater. Chem. Phys.* 122 (2010) 325.
16. I.B. Obot, N.O. Obi-Egbedi, *Corr. Sci.* 52 (2010) 282.
17. Y. Abboud, A. Abourriche, T. Saffaj, M. Berrada, M. Charrouf, A. Bennamara, N. Al Himidi, H. Hannache, *Mater. Chem. Phys.* 105 (2007) 1.
18. N. Saoudi, A. Bellaouchou, A. Guenbour, A. Ben Bachir, E.M. Essassi, M. El Achouri, *Bulletin of Materials Science*, 33 (2010) 313.
19. I .L. Finar, *J. Chem. Soc.* (1955) 1205.
20. S.-K. Lin, *Molecules*, 1 (1996) 37.
21. R. Touzani, T. Ben-Hadda, S. El Kadiri, A. Ramdani, O. Maury, H. Le Bozec, L. Toupet, P. H. Dixneuf, *New J. Chem.* 25 (2001) 391.

22. M. J. Waring, T. Ben-Hadda, A.T. Kotchevar, A. Ramdani, R. Touzani, S. El Kadiri, A. Hakkou, M. Bouakka, T. Ellis, *Molecules*, 7 (2002) 641.
23. I. Bouabdallah, I. Zidane, R. Touzani, F. Malek, M. El Kodadi, A. Ramdani, *Molbank* (2004) M384-M385.
24. I. Bouabdallah, I. Zidane, R. Touzani, B. Hacht, A. Ramdani, *ARKIVOC*. 10 (2006) 77.
25. M. Bouklah, A. Attayibat, S. Kertit, A. Ramdani, B. Hammouti, *Appl. Surf. Sci.* 242 (2005) 399.
26. A.S. Fouda, H. A. Mostafa, F. El-Taib, G.Y. Elewady, *Corros. Sci.* 47 (2005) 1988.
27. K. Tebbji, H. Oudda, B. Hammouti, M. Benkaddour, M. El Kodadi, A. Ramdani, *Colloids Surf.* 259 (2005) 143.
28. M. A. Amin, M. M. Ibrahim, *Corros. Sci.* 52 (2011) 873.
29. L. Elkadi, B. Mernari, M. Traisnel, F. Bentiss, M. Lagrenée, *Corros. Sci.* 42 (2000) 703.
30. E. McCafferty, N. Hackerman, *J. Electrochem. Soc.* 119 (1972) 146.
31. P. Li, J.Y. Lin, K.L. Tan, J.Y. Lee, *Electrochim Acta*, 42 (1998) 605.
32. S.S. Abdel Rehim, O.A. Hazzazi, M.A. Amin, K.F. Khaled, *Corros. Sci.* 50 (2008) 2258.
33. J.O. M. Bockris, A.K.N. Modern Electrochemistry. Vol. 2, Macdonald Ltd., London, (1970) P. 772
34. F. Bentiss, M. Traisnel, L. Gengembre, M. Lagrenée, *Appl. Surf. Sci.* 152 (1999) 237.
35. O. K. Abiola, J.O.E. Otaigbe, *Int. J. Electrochem. Sci.*, 3 (2008) 191.
36. E.E. Ebenso, I. B. Obot, L. C. Murulana, *Int. J. Electrochem. Sci.*, 5 (2010) 1574.
37. L.M. Rodriguez-Valdez, A. Martinez-Villafane, D. Glossman-Matnik, *J. Mol. Struct. THEOCHEM* 713 (2005) 65.
38. J.G.N. Thomas, in: Proc. 5th Europ. Symp. on Corrosion Inhibitors, Ann. Univ. Ferrara, Italy, 1980, 1981, pp. 453.
39. W. J. Lee, *Mat. Sci. Eng. A* , 348 (2003) 217.
40. K.F.Khaled , Amin MA , *Corros. Sci.* 51 (2009) 2098.
41. N.A. Al-Mobarak K. F., Khaled, K. M., Abdel-Azim, *J. Mater. Environ. Sci.* 1 (2010) 9.